

Next generation of high power phase-controlled thyristor and rectifier diode

Nino Degiampietro, Zuzana Ptakova, Christian Winter – Hitachi Energy Switzerland Ltd.

PCT and rectifier diodes to support the demand for more efficiency

Power efficiency is a key enabler towards a greener future. Especially for industry, where the demand for electrical energy is enormous, improved power efficiency can significantly impact the environment towards a sustainable future.

Hitachi Energy has developed a new generation of phase-controlled thyristors (PCT) and rectifier diodes by using its latest technologies in the wafer production line to maximize performances, increase efficiency and enhance the cost per device's performance ratio. This white paper provides an insight into this new generation focusing on a PCT and a rectifier diode both rated at 6500 V in the N-housing (100 mm pole piece diameter, 35 mm height).

Introduction

Today, the PCT is a key component in high-power rectifiers, power supplies, motor drives, power quality systems, hydro pumping, hydrogen electrolysis, HVDC, and more. It is the number one choice in high power applications where the highest performance, reliability, and low conduction losses are required (Fig. 1). In some less sophisticated applications of high-power rectifiers or power supplies, the

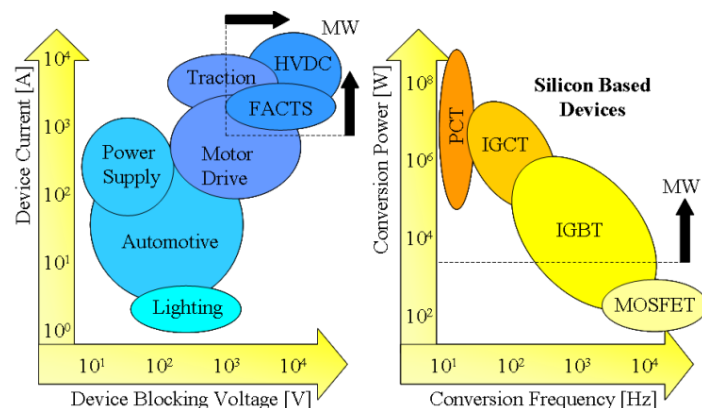


Fig. 1: Power semiconductor devices and applications [1]

rectifier diode, providing minimal conduction losses, is also a desired solution in today's industry.

Hitachi Energy has developed a new platform for PCT and rectifier diodes to support the demand for more efficiency, enabling one step more towards sustainability. In this paper, the new platform is presented by focusing on the first two pilot products: a PCT and a rectifier diode (Fig. 2).

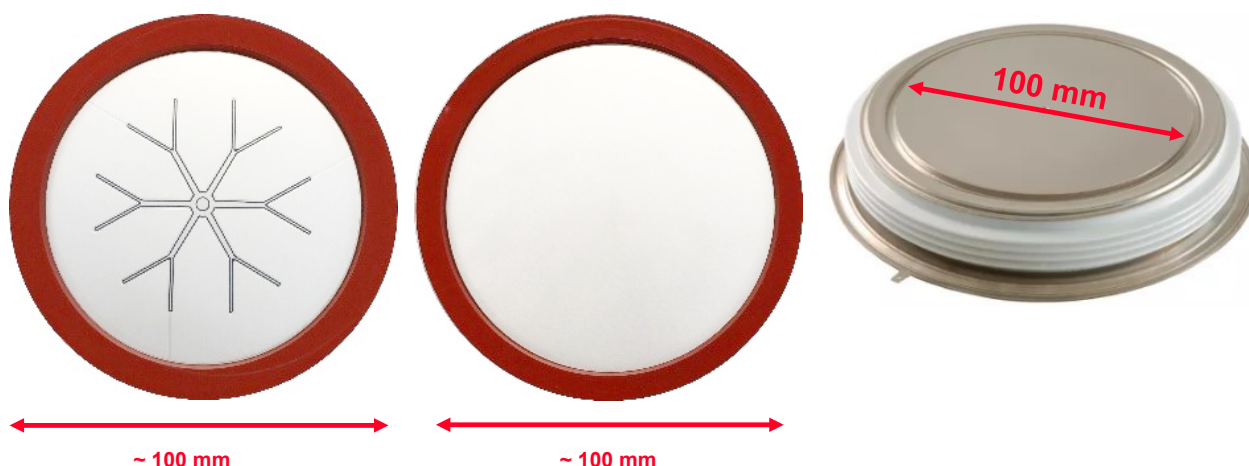


Fig. 2: Fabricated wafers of 6.5 kV PCT (left) rectifier diode (center) and encapsulated device (right)

Device design

Silicon Wafer

PCT and rectifier diodes for an industrial application aim for maximized junction temperature, maximized rated forward and surge current. Although the outline of the new products is identical to the previous generation, which allows a one-to-one replacement from the mechanical point of view, the inside of the devices differs drastically. In order to push the device ratings, major aspects of the devices were changed:

- Wafer Size

The diameter of the device was increased to the maximum with respect to the available space inside the N-housing. This leads to an increase in the active area of 15 %.

- Maximum virtual junction temperature

The maximum junction temperature is increased by 10 K for both

semiconductors to increase the output power. In order to withstand the increased thermal loads (e.g., higher leakage current during blocking), major changes with regards to the silicon wafer were needed. First, a positive-negative beveled junction termination was introduced. On top of that, the junction termination is coated with the latest passivation technology made of amorphous hydrogenated carbon (also known as DLC). Combining this junction termination design with the passivation layer boosts the blocking performance and provides outstanding robustness at a high temperature. By introducing the positive beveled junction termination, the depth of the anode junction could be reduced (Fig. 3), which allows the silicon thickness to be reduced and the on-state performance enhanced.

- Low-temperature bonding

The low-temperature bonding of the silicon wafer to the adjacent molybdenum on the anode side was introduced to the thyristors and rectifier diodes of this new platform. This brings multiple benefits:

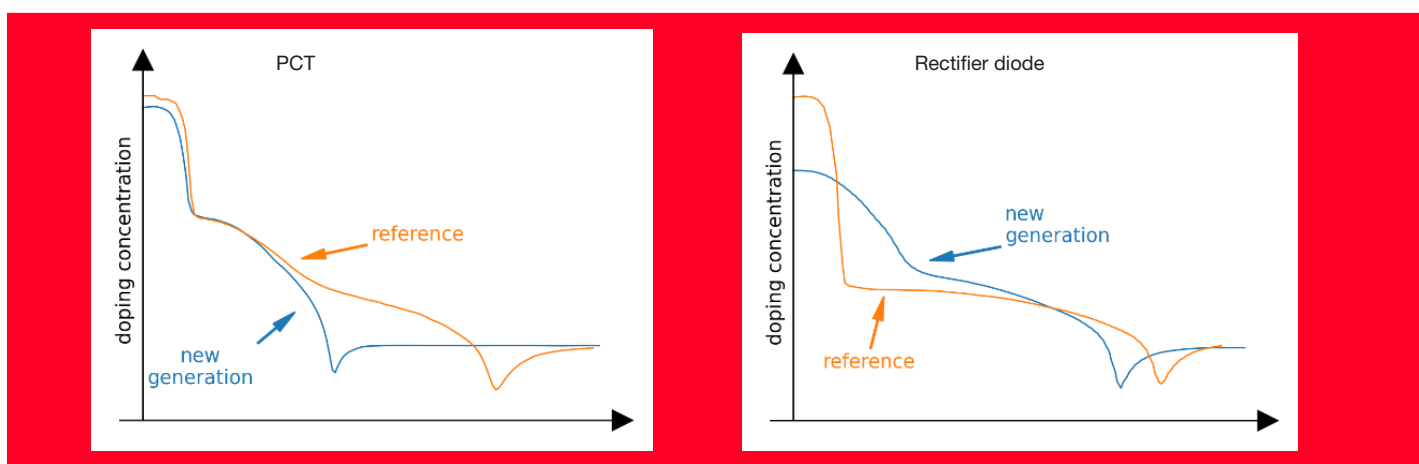


Fig. 3: The doping profile of the anode of the PCT (left) and the rectifier diode (right)

The silicon wafer is cooled up to the very edge. This additionally helps to withstand the increased thermal loads besides the adaptations and modifications of the silicon wafer. Furthermore, the bonding eliminates the dry interface between molybdenum and silicon wafer leading to a lower thermal resistance between those two parts. As a result, the cooling of the silicon wafer is intensified, which contributes to a reduction of the thermal resistance between the junction of the silicon wafer and the packaging case.

Packaging

The introduction of silicon-molybdenum bonding for PCTs and rectifier diodes comes with additional packaging changes. As visualized in Fig. 4, the free-floating (FF) technology, present with the existing generation of PCT and rectifier diodes, is characterized by a symmetric packaging design. The dimensions of the adjacent molybdenum discs and copper pole pieces are identical for the anode and

the cathode side. In contrast, the packaging of the bonded devices differs significantly. As mentioned above, the diameter of the anode pole piece has been increased to match the diameter of the wafer, whereas the cathode pole piece was adapted to fit the cathode side's active area of the silicon wafer. Due to the bonding on the anode side, the thickness of the cathode molybdenum was reduced and substituted by copper. Hence, another improvement of the thermal and electrical resistances results are due to copper's higher electrical and thermal conductivity. However, as a result of the asymmetry, the thermal resistances of the anode and the cathode are not equal.

Case non-rupture current capability

The two new products are offered in a second type of packaging, providing enhanced case non-rupture current capability (I_{RSMC}). The such called X-housing (Fig. 5) is based on the new N-housing for bonded devices (Fig. 4 right) and is additionally equipped with a steel flange (yellow), a polymer-based ring (blue), and a silicone O-ring (black)

N-housing of free-floating technology

New N-housing with bonded technology

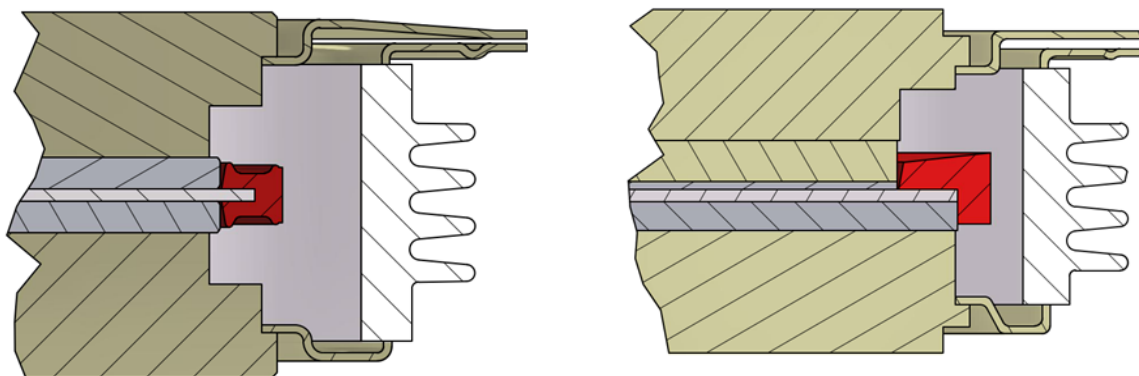


Fig. 4: Cross-section of the N-housing for the free-floating technology (left) and bonded technology (right)

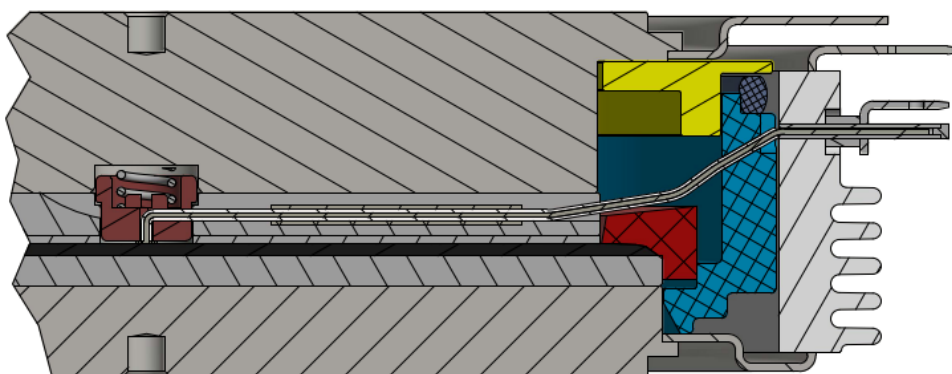


Fig. 5: Cross-section of the X-housing providing enhanced I_{RSMC} capability

clamped in-between. In addition, the anode pole piece was shrunk-en, and the ceramic dimensions were increased to the diameter of the cathode flange to provide enough space for the steel flange and

	5STP 26N6500 [2] free floating	5STP 40N6500 [3] bonded	5STP 40X6500 bonded, I _{RSMC}	5SDD 50N5500 [4] free-floating	5SDD 57N6500 [5] bonded	5SDD 57X6500 bonded, I _{RSMC}
R _{th(j-c),DC} Anode	11.4 K kW ⁻¹	8.5 K kW ⁻¹ - 25 %	7.2 K kW ⁻¹ - 37 %	11.4 K kW ⁻¹	8.5 K kW ⁻¹ - 25 %	7.2 K kW ⁻¹ - 37 %
R _{th(j-c),DC} Cathode	11.4 K kW ⁻¹	11.0 K kW ⁻¹ - 3 %	13.5 K kW ⁻¹ + 18 %	11.4 K kW ⁻¹	10.4 K kW ⁻¹ - 9 %	13.0 K kW ⁻¹ + 14 %
R _{th(j-c),DC}	5.7 K kW ⁻¹	4.8 K kW ⁻¹ - 16 %	4.7 K kW ⁻¹ - 18 %	5.7 K kW ⁻¹	4.7 K kW ⁻¹ - 18 %	4.6 K kW ⁻¹ - 19 %

Tab. 1: Summary of thermal resistances

the polymer-based ring.
The thinner anode pole piece intensifies the thermal resistance imbalance, but the significant improvement with respect to the refer-ences is maintained as shown in Tab. 1.
This second type of packaging provides an I_{RSMC} rating of 95 kA at a

10 ms sinusoidal single pulse. The I_{RSMC} was assessed based on the standard IEC IEC60747-6. The devices were damaged mechanically on the junction termination before the I_{RSMC} testing. During testing, a high-speed camera was used to track at which current level the her-

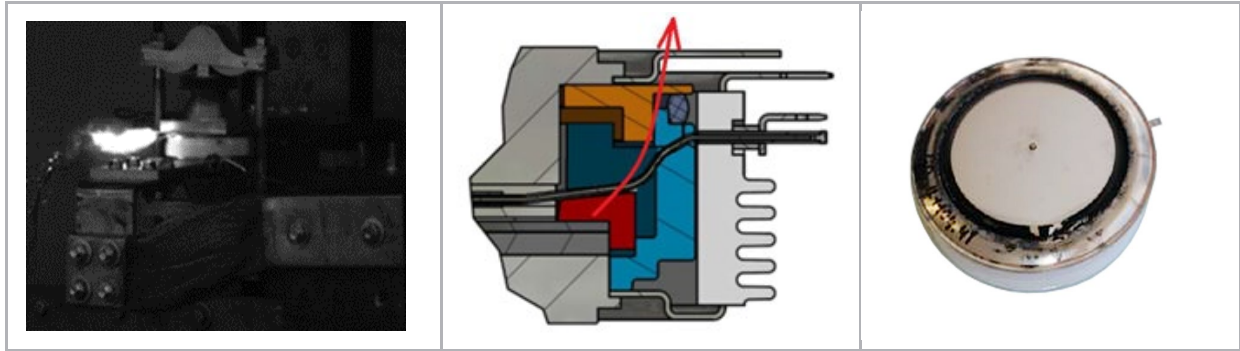


Fig. 6: I_{RSMC} testing – high-speed camera image and failure pattern when exceeding the limit

miticity of the packaging was damaged and plasma escaped. In Fig. 6, the results of the I_{RSMC} verification are shown. The packaging was designed to ensure that the plasma escapes at the cathode flange when exceeding the I_{RSMC} limit to ensure that the ceramic remains undamaged.

Device performance

Technology curve

The trade-off between on-state voltage drop and reverse recovery charge of the new generation compared to the previous generation, and selected competitors are shown in Fig. 7. The static losses at constant reverse recovery charge were decreased by 3 % for the PCT. This increases current density to 62.3 A/cm² (+11 %) in

combination with the reduced thermal resistance and the increased junction temperature. The situation on the diode is similar: the static losses are reduced by 3 %, and the current density is increased to 79.7 A/cm² (+ 8 %). Thus, a significant improvement regarding rated forward current was achieved in comparison to the previous generation.

Surge current capability

The bonding technology is one of the key factors to withstand a higher junction temperature to avoid thermal runaway under blocking conditions. On the other hand, this technology enables a significantly enhanced performance at surge conditions. The surge current (PCT: I_{TSM}, Rectifier diode: I_{FSM}) capability was assessed thoroughly during the product development. The main result in the case of the rectifier diode is visualized in Fig. 8, which shows the last peak current value of the surge current testing before the device got destroyed. The lowest last pass in surge current testing of the new rectifier diode

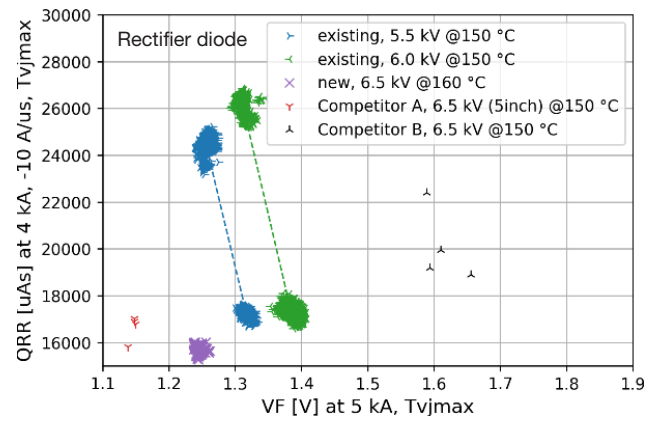
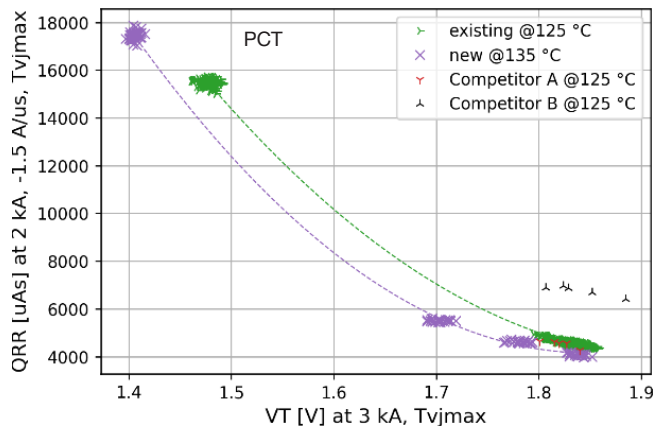


Fig. 7: Reverse recovery charge Q_{RR} vs. on-state voltage drop of the PCT (left) and rectifier diode(right) in comparison to the previous generation and selected competitors. Q_{RR} measured at $V_R = 200$ V for PCT and Rectifier diode.

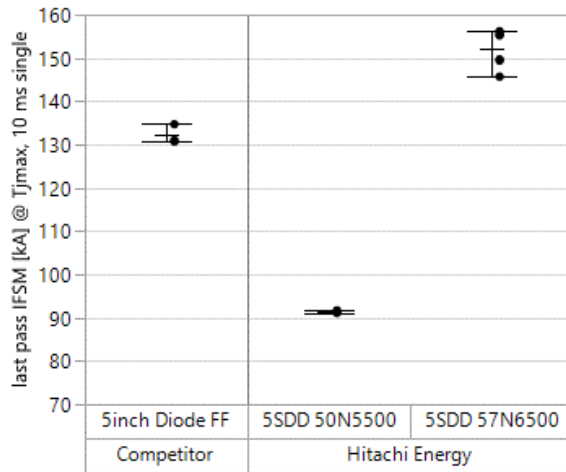


Fig. 8: Surge current testing results of the rectifier diode (5SDD 57N6500) in comparison to the previous generation (5SDD 50N5500) and the 5inch competitor device

Ratings

The current ratings of the devices mainly depend on the forward voltage drop, the device's thermal resistance, and the maximum operating temperature. As described in the previous sections, all three aspects were enhanced, leading to improved ratings. The forward current rating is increased in the range 25 % to 35 % and the surge current ratings by 12 % to 15 %, respectively. A summary of all relevant ratings of the new products compared to the previous generation is listed in Tab. 2.

	Device	$V_{DSM/RSM}$ $V_{DRM/RRM}$	I_{TAVM}	$T_{vj,max}$	$R_{th(j-c), DC}$	I_{TSM} / I_{FSM}
PCT	New: 5STP 40N6500* [3]	6500 V	3780 A +31 %	135 °C +10 K	4.8 K kW ⁻¹ -16 %	75 kA +15 %
	New: 5STP 40X6500*	6500 V	3780 A +31 %	135 °C +10 K	4.7 K kW ⁻¹ -17 %	75 kA +15 %
	Ref.: 5STP 26N6500 [2]	6500 V	2810 A	125 °C	5.7 K kW ⁻¹	65 kA
Rectifier diode	New: 5SDD 57N6500* [5]	6500 V +500 V ... 1500 V	5700 A +25 % / +35 %	160 °C +10 K	4.7 K kW ⁻¹ -18 %	82 kA +12 % / +15 %
	New: 5SDD 57X6500*	6500 V +500 V ... 1500 V	5700 A +25 % / +35 %	160 °C +10 K	4.6 K kW ⁻¹ -19 %	82 kA +12 % / +15 %
	Ref. 1: 5SDD 50N5500 [4]	5500 V 5000 V	4570 A	150 °C	5.7 K kW ⁻¹	73 kA
	Ref. 2: 5SDD 50N6000 [6]	6000 V	4210 A	150 °C	5.7 K kW ⁻¹	71.2 kA

Tab. 2: Key device ratings in comparison to the previous generation (* = Preliminary data sheet values)

is around 145 kA at a 10 ms sinusoidal single pulse. This equals a surge current improvement compared to the previous generation of almost 60 %. The surge current capability of the larger device from competitor A has been exceeded while being characterized by a lower on-state voltage drop. The enhanced surge current capability is attributed to the silicon design and the bonding technology.

Conclusions

The key numbers and facts of the first two products of Hitachi Energy's new platform of high-power PCT and rectifier diodes were presented. An improvement in the rated current of 30 % was achieved by maintaining the device's footprint, allowing this generation of devices to compete with the next larger size and elevating power efficiency to a new level. Applications, which will be using the devices of this latest generation, will benefit massively by becoming more powerful and cost-efficient.

References

[1] M. T. Rahimo, "Ultrahigh voltage semiconductor power devices for grid application," in 2010 International Electron Devices Meeting, pp. 13.4.1-13.4.4, 2010.

[2] ABB Power Grids Switzerland Ltd Semiconductors, "Datasheet 5STP 26N6500," 20 March 2020. [Online]. Available: <https://search.abb.com/library/Download.aspx?DocumentID=5SYA1001&LanguageCode=en&DocumentPartId=&Action=Launch>.

[3] ABB Power Grids Switzerland Ltd Semiconductors, "Preliminary Datasheet 5STP 40N6500," 01 February 2021. [Online]. Available: <https://search.abb.com/library/Download.aspx?DocumentID=5SYA1086&LanguageCode=en&DocumentPartId=&Action=Launch>.

[4] ABB Power Grids Switzerland Ltd Semiconductors, "Datasheet 5SDD 50N5500," 02 January 2017. [Online]. Available: <https://search.abb.com/library/Download.aspx?DocumentID=5SYA1169-00&LanguageCode=en&DocumentPartId=&Action=Launch>.

[5] ABB Power Grids Switzerland Ltd Semiconductors, "Preliminary Datasheet 5SDD 57N6500," 21 January 2021. [Online]. Available: <https://search.abb.com/library/Download.aspx?DocumentID=5SYA1190&LanguageCode=en&DocumentPartId=&Action=Launch>.

[6] ABB Power Grids Switzerland Ltd Semiconductors, "Datasheet 5SDD 50N6000," 01 June 2017. [Online]. Available: <https://search.abb.com/library/Download.aspx?DocumentID=5SYA%201188&LanguageCode=en&DocumentPartId=&Action=Launch>.